

1 Supplemental material submitted for the paper:

2 **Long-term surface pCO₂ trends from observations and models**

3 Jerry F. Tjiputra^{1*}, Are Olsen^{2,1}, Laurent Bopp³, Andrew Lenton⁴, Benjamin Pfeil²,
4 Tilla Roy³, Joachim Segschneider⁵, Ian Totterdell⁶, and Christoph Heinze^{2,1}

5 ¹Bjerknes Centre for Climate Research, Uni Research Climate, Bergen, Norway

6 ²Geophysical Institute, University of Bergen and Bjerknes Centre for Climate Research,
7 Bergen, Norway

8 ³IPSL/LSCE, UMR8212, CNRS-CEA-UVSQ, Gif sur Yvette, France

9 ⁴Centre for Australian Weather and Climate research, CSIRO, Marine and Atmospheric
10 Research, Hobart, Tasmania, Australia

11 ⁵Max Planck Institute for Meteorology, Bundesstr. 53, Hamburg, Germany

12 ⁶Met Office, Hadley Centre, Exeter, United Kingdom

13

*Corresponding author

Email: jerry.tjiputra@uni.no

14 **1 Introduction**

15 In this supplemental document, we briefly describe the five Earth system model used and
16 analyzed in our paper. Additionally, we also present plots of the long-term change surface
17 salinity from each model, which are not included but support the analysis presented in
18 the paper.

19 **2 Description of the models**

20 **2.1 NorESM1-ME**

21 The Norwegian Earth System Model (NorESM1-ME) was developed in Norway in
22 collaboration with researchers from the National Center for Atmospheric Research at the
23 United States. Some of the NorESM1-ME components are therefore based on the version
24 4 of the Community Climate System Model (CCSM4), namely the atmospheric general
25 circulation (Community Atmospheric Model, CAM4), land (Community Land Model,
26 CLM4), and sea-ice (Community, CICE4) components (Gent et al., 2011). The
27 atmospheric chemistry in CAM4 was modified following Seland et al. (2008). The ocean
28 general circulation is based on the Miami Isopycnic Coordinate Ocean Model (MICOM),
29 coupled together with the Hamburg Oceanic Carbon Cycle (HAMOCC5) model
30 (Assmann et al., 2010). HAMOCC5 consists of an NPZD-type ecosystem model, where
31 the phytoplankton growth is co-limited by nitrate, phosphate, and dissolved iron. For the
32 simulations analyzed here, there is no riverine influx of biogeochemical tracers. For the
33 air-sea gas exchange, the steady winds gas transfer rate from Wanninkhof (1992) is used.
34 The inorganic carbon chemistry follows the Ocean Carbon Model Intercomparison
35 Project (OCMIP) protocols. In addition to the above modules, NorESM-ME also adopts
36 the CCSM4 coupler (CPL7), which handles the communication exchanges between the

37 different components. More detailed description of the model is available in Tjiputra et
38 al. (2013).

39 **2.2 HadGEM2-ES**

40 The Hadley Centre Earth system model (HadGEM2-ES) is based on the HadGEM1
41 (Johns et al., 2006) with further improvement including ocean and terrestrial
42 biogeochemistry, interactive atmospheric chemistry, and aerosol components (Collins et
43 al., 2011). The ocean carbon cycle component of HadGEM2-ES, the Diat-HadOCC, is an
44 improved version of the original HadOCC model (Palmer and Totterdell, 2001), which
45 simulates multi-functional groups of phytoplankton, nitrogen cycle, marine
46 dimethylsulphide (DMS) emission, and multi-nutrient limitations of silica and iron. As
47 with the NorESM1-ME, the HadGEM2-ES does not include biogeochemical tracers in the
48 riverin fluxes. The land carbon cycle is represented by the MOSES2 land surface scheme,
49 which implements exchange of water, energy, and carbon with the land-atmosphere
50 interface. It also includes the TRIFFID dynamic global vegetation model, simulating five
51 plant functional types (Cox, 2001).

52 **2.3 IPSL-CM5A-LR**

53 The latest version of the IPSL ESM includes improvements in tropospheric chemistry,
54 aerosols, and online interactions with land vegetation. The atmospheric and oceanic
55 general circulation models are LMDZ (Hourdin et al., 2006) and NEMOv3.2 (Madec,
56 2008), respectively. The land surface model is represented by ORCHIDEE (Krinner et
57 al., 2005) and the ocean carbon cycle is PISCES (Aumont and Bopp, 2006). PISCES
58 simulates multi-functional groups of phytoplankton and zooplankton, with phytoplankton
59 growth rates being limited by several nutrients and availability of light. PISCES also
60 differentiates between small and large sinking particles, by simulating different vertical

61 sinking speeds. The air-sea gas exchange parameterization also follows the quadratic
62 wind speed formulation by Wanninkhof (1992). The IPSL-CM5A-LR uses climatological
63 riverine fluxes of DIC, DOC and POC. It assumes that all POC is lost in the estuaries,
64 and that DOC is labile and thus remineralized.

65 **2.4 MPI-ESM-LR**

66 The Max Planck Institute for Meteorology’s Earth System Model (MPI-ESM) was
67 developed in Hamburg, Germany. It consists of the atmospheric general circulation
68 models ECHAM6 and the oceanic z-layer model MPIOM (Roeckner et al., 2003;
69 Jungclaus et al., 2006). The land surface model, JSBACH, simulates energy, water,
70 momentum, and CO₂ fluxes between the land and atmosphere (Raddatz et al., 2007). In
71 addition, dynamical vegetation with 12 plant functional types is also included in the
72 model. MPI-ESM-LR uses HAMOCC5 (Maier-Reimer et al., 2005) as its ocean carbon
73 cycle component. Riverine input of DIC/ALK are set similar to the losses to the
74 sediment (CaCO₃) and to DOC to balance the loss of organic carbon. The riverine input
75 rates are determined by diagnosing the loss to the sediment over a few hundred years in
76 the control/spinup run. A more detailed description of HAMOCC as used in CMIP5 can
77 be found in Ilyina et al. (2013).

78 **2.5 CESM1**

79 The Community Earth System Model (CESM1) is a fully-coupled, global climate model
80 consisting of land, atmosphere, ocean, and sea-ice components (Gent et al., 2011). The
81 marine ecosystem module utilizes multiple phytoplankton functional groups and a single
82 zooplankton class. Phytoplankton growth is controlled by temperature, light, and
83 available nutrients (N, P, Si, Fe). The behavior of the marine carbon cycle is documented
84 by Long et al. (2013). The land surface model, CLM4 (Lawrence et al., 2012) includes a

85 biogeochemical module with coupled carbon-nitrogen dynamics (Thornton et al., 2009).

86 **3 Regional pCO₂ trends using varying starting date**

87 Figure S1 shows the models simulated surface pCO₂ trend in each of the 14 regions. It
88 highlights how the computed pCO₂ trends change when different starting period is used.
89 The figure was motivated by the fact that most of the observations are biased toward
90 recent periods with generally poor coverage prior to the 1990s. The figure shows that in
91 nearly all regions and all models, the pCO₂ trends increase when the starting year is
92 closer to the present day (e.g., trends for the 1990-2011 is stronger than 1970-2011
93 periods). This result is consistent with the fact that atmospheric CO₂ concentration also
94 grows at a faster rate in the later part of 1970-2011 period.

95 **4 Spatial changes in sea surface salinity**

96 Figure S2 shows the long-term change in the sea surface salinity (SSS) for the
97 contemporary period and the last 40-yrs of this century under RCP8.5 scenario as
98 simulated by the five ESMs used in this study.

99 **References**

- 100 Assmann, K. M., Bentsen, M., Segschneider, J. and Heinze, C. 2010. An isopycnic ocean
101 carbon cycle model, *Geosci. Model Dev.*, **3**, 143–167, 2010.
- 102 Aumont, O. and Bopp, L. 2006. Globalizing results from ocean in situ iron fertilization
103 studies, *Global Biogeochem. Cycles*, **20**, GB2017, doi:10.1029/2005GB002591.
- 104 Collins, W. J., Bellouin, N., Doutriaux-Boucher, M., Gedney, N., Halloran, P. and

105 co-authors. 2011. Development and evaluation of an Earth-system model - HadGEM2,
106 *Geosci. Model Dev.*, **4**, 1051–1075.

107 Cox, P. M. 2001. Description of the TRIFFID Dynamic Global Vegetation Model,
108 *Technical Note 24*, Hadley Centre, Met Office, 17 pp.

109 Gent, P. R., Danabasoglu, G., Donner, L. J., Holland, M. M., Hunke, E. C. and
110 co-authors. 2011. The Community Climate System Model Version 4, *J. CLimate*, **24**,
111 4973–4991, doi:<http://dx.doi.org/10.1175/2011JCLI4083.1>.

112 Hourdin, F., Musat, I., Bony, S., Braconnot, P., Cordon, F. and co-authors. 2006. The
113 LMDZ4 general circulation model: climate performance and sensitivity to
114 parameterized physics with emphasis on tropical convection, *Clim. Dyn.*, **27**, 787–813.

115 Ilyina, T., Six, K. D., Segschneider, J., Maier-Reimer, E., Li, H. and co-authors. 2013.
116 The global ocean biogeochemistry model HAMOCC: Model architecture and
117 performance as component of the MPI-Earth System Model in different CMIP5
118 experimental realizations. *Journal of Advances in Modeling Earth Systems*.
119 doi:10.1002/jame.20017.

120 Johns, T. C., Durman, C. F., Banks, H. T., Roberts, M. J., McLaren, A. J. and
121 co-authors. 2006. The new Hadley Centre Climate Model (HadGEM1): Evaluation of
122 coupled simulations, *J. Climate*, **19**, 1327–1353.

123 Jungclaus, J. H., Keenlyside, N., Botzet, M., Haak, H., Luo, J. J. and co-authors. 2006.
124 Ocean circulation and tropical variability in the coupled model ECHAM5/MPI-OM, *J.*
125 *Climate*, **19**, 3952–3972, 2006.

126 Krinner, G., Viovy, N., de Noblet-Ducoudré, N., Ogée, J., Polcher, J. and co-authors.
127 2005. A dynamic global vegetation model for studies of the coupled

128 atmosphere-biosphere system, *Global Biogeochem. Cycles*, *19*, GB1015,
129 doi:10.1029/2003GB002199.

130 Long, M. C., Lindsay, K., Peacock, S., Moore, J. K. and Doney, S. C. 2013.
131 Twentieth-century oceanic carbon uptake and storage in CESM1(BGC), *J. Climate*,
132 **26(18)**, doi:10.1175/JCLI-D-12-00184.1.

133 Lawrence, D. M., Oleson, K. W., Flanner, M. G., Fletcher, C. G., Lawrence, P. J. and
134 co-authors. 2012. The CCSM4 land simulation, 1850–2005: Assessment of surface
135 climate and new capabilities, *J. Climate*, **25(7)**, 2240–2260,
136 doi:10.1175/JCLI-D-11-00103.1.

137 Madec, G. 2008. NEMO ocean engine, *Note du Pole de modélisation*, **27**, ISSN No:
138 1288-1619, Institut Pierre-Simon Laplace (IPSL), Gif-sur-Yvette, France.

139 Maier-Reimer, E., Kriest, I., Segschneider, J., and Wetzel, P. 2005. The HAMburg Ocean
140 Carbon Cycle Model HAMOCC5.1 - Technical Description Release 1.1, *Berichte zur*
141 *Erdsystemforschung 14*, ISSN 1614-1199, Max Planck Institute for Meteorology,
142 Hamburg, Germany, 50pp.

143 Palmer, J. R. and Totterdell, I. J. 2001. Production and export in a global ocean
144 ecosystem model, *Deep-Sea Res. I*, *48*, 1169–1198.

145 Raddatz, T. J., Reick, C. H., Knorr, W., Kattge, J., Roeckner, E. and co-authors. 2007.
146 Will the tropical land biosphere dominate the climate–carbon cycle feedback during the
147 twenty-first century?, *Climate Dynamics*, **29**, 565–574, doi:10.1007/s00382-007-0247-8.

148 Rayner, N. A., Parker, D. E., Horton, E. B., Folland, C. K., Alexander, L. V. and
149 co-authors. 2003. Global analyses of sea surface temperature, sea ice, and night marine

150 air temperature since the late nineteenth century, *J. Geophys. Res. Vol.*, **108**,
151 doi:10.1029/2002JD002670.

152 Roeckner, E., Bäuml, G., Bonaventura, L., Brokopf, R., Esch, M. and co-authors. 2003.
153 The atmospheric general circulation model ECHAM5. Part I: Model description,
154 *Report 349*, Max Planck Institute for Meteorology, Hamburg, 127 pp.

155 Seland, Ø., Iversen, T., Kirkevåg, A. and Storelvmo, T. 2008. Aerosol–climate
156 interactions in the CAM-Oslo atmospheric GCM and investigation of associated basic
157 shortcomings, *Tellus*, **60A**, 459–491.

158 Thornton, P. E., Doney, S. C., Lindsay, K., Moore, J. K., Mahowald, N. and co-authors.
159 2009. Carbon-nitrogen interactions regulate climate-carbon cycle feedbacks: results
160 from an atmosphere-ocean general circulation model, *Biogeosciences*, **6(10)**,
161 2099–2120, doi:10.5194/bg-6-2099-2009.

162 Tjiputra, J. F., Roelandt, C., Bentsen, M., Lawrence, D. M., Lorentzen, T. and
163 co-authors. 2013. Evaluation of the carbon cycle components in the Norwegian Earth
164 System Model (NorESM), *Geosci. Model Dev.*, **6**, 301-325, doi:10.5194/gmd-6-301-2013.

165 Wanninkhof, R. 1992. A relationship between wind speed and gas exchange over the
166 ocean, *J. Geophys. Res.*, **97**, 7373–7382.

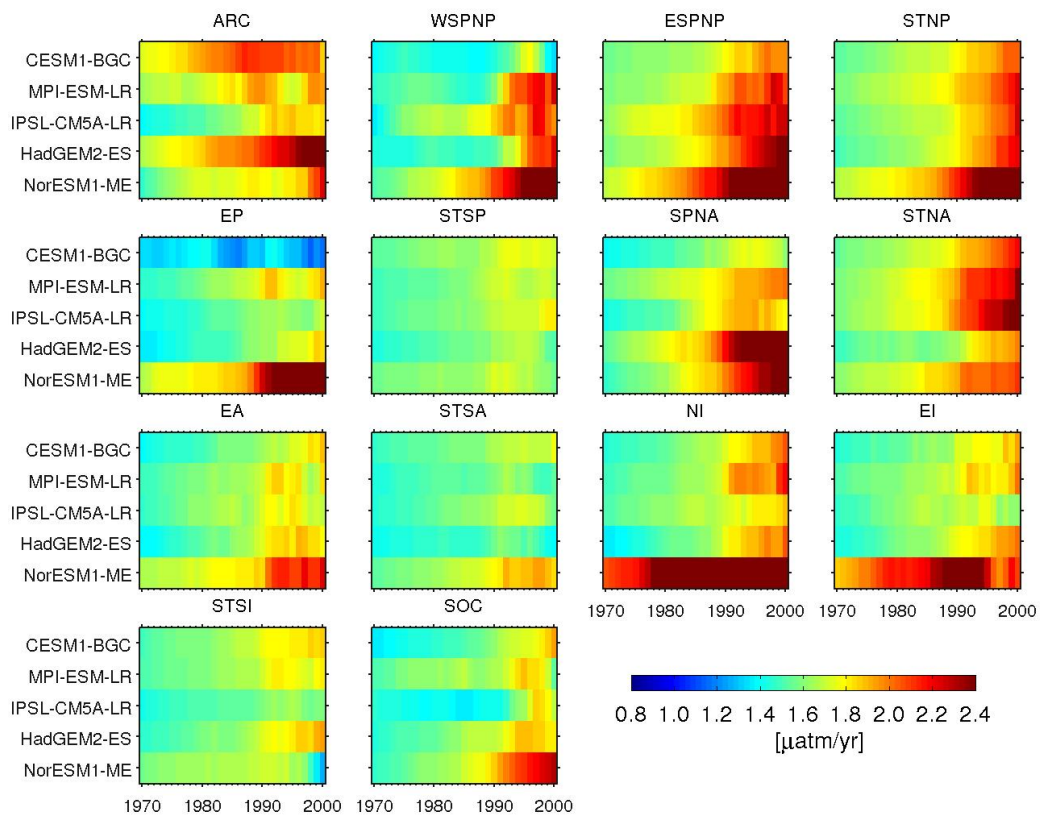


Figure S1. Mean regional trends of surface pCO₂ simulated by five ESMs for the periods starting from years given in x-axis and ending at year 2011. Units are in [$\mu\text{atm yr}^{-1}$].

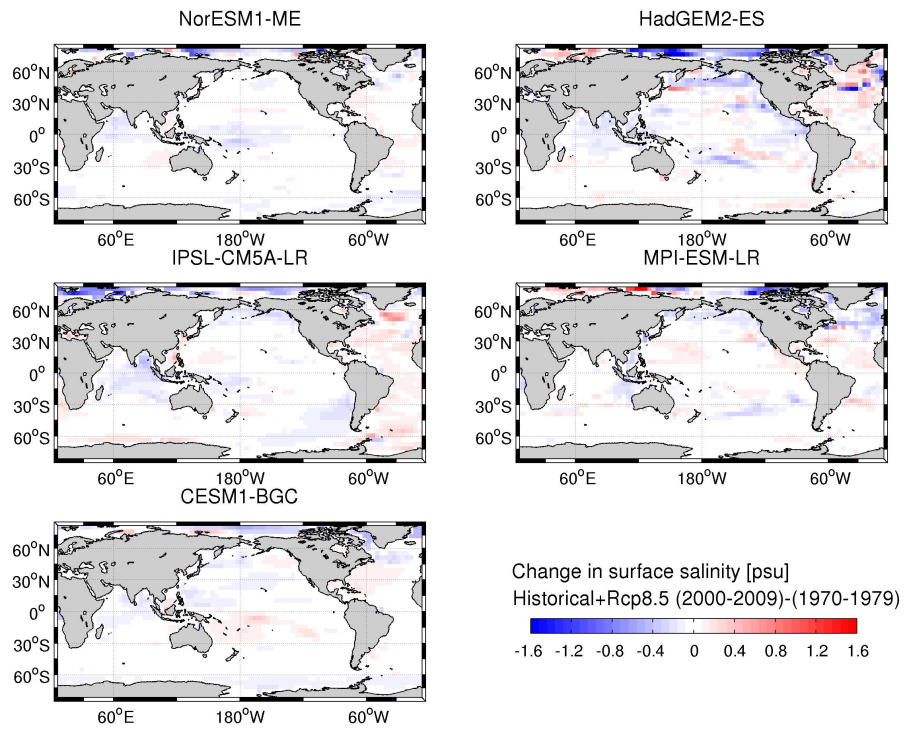


Figure S2. Simulated mean change in sea surface salinity by the NorESM1-ME, HadGEM2-ES, IPSL-CM5A-LR, MPI-ESM-LR, and CESM1-BGC models for the contemporary period: $\text{mean}(2000-2009) - \text{mean}(1970-1979)$. Units are in [psu].

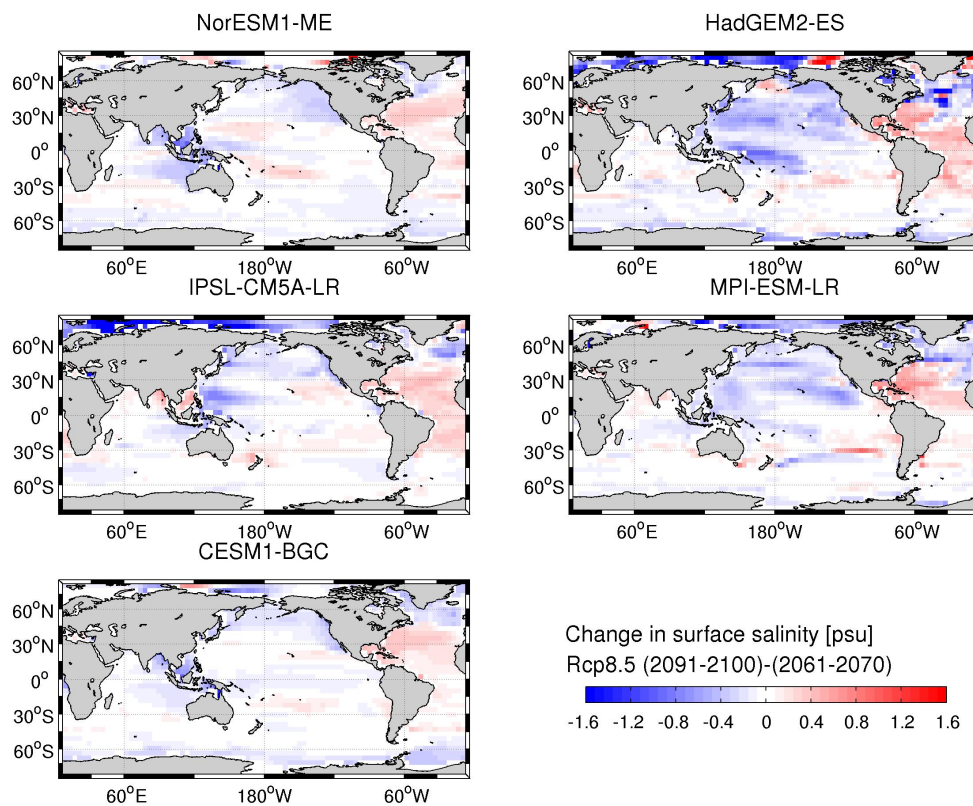


Figure S3. Simulated mean change in sea surface salinity by the NorESM1-ME, HadGEM2-ES, IPSL-CM5A-LR, MPI-ESM-LR, and CESM1-BGC models for the last 40-yr period of this century under RCP8.5 scenario: mean(2091–2100) minus mean(2061–2070). Units are in [psu].